Research Article Vol. 30, No. 13 / 20 Jun 2022 / Optics Express 23499

Optics EXPRESS

Full-color micro-display by heterogeneous integration of InGaN blue/green dual-wavelength and AlGaInP red LEDs

PEIAN LI, XU ZHANG, LONGHENG QI, AND KEI MAY LAU*

Photonics Technology Center, Department of Electronic and Computer Engineering, The Hong Kong University of Science and Technology, Clear Water Bay, Hong Kong
*eekmlau@ust.hk

Abstract: A full-color micro-display via bonding of a InGaN blue/green dual-wavelength light-emitting diode (LED) array and a AlGaInP red LED array is demonstrated. The micro-display has a 120 µm pixel pitch, and each pixel consists of 40 µm × 120 µm red/green/blue (R/G/B) subpixels. The red LED array was integrated with the blue/green dual-wavelength LED array by Au/In flip-chip bonding to achieve full-color emission. Full-color images presented by the micro-display have high brightness and a wide color gamut. This heterogeneous integration technology using conventional LED materials shows the feasibility of a cost-effective approach for reliable high-performance full-color LED micro-displays in virtual reality (VR) and augmented reality (AR) devices.

1. Introduction

Micro-display technologies have received much attention in recent years with the fast development of virtual reality (VR) and augmented reality (AR) [1]. Micro-displays are typically small near-eye displays (NEDs) essential for VR/AR applications [2]. Inorganic light-emitting diodes (LEDs) are recognized as an appealing technology for future micro-displays due to their better performances in the aspects of brightness, power consumption, response time and lifespan [3–6] compared with the more mature liquid crystal (LC) and organic LED (OLED) technologies.

In the past two decades, researchers have made remarkable progress on monochromatic LED micro-displays using monolithic fabrication. Numerous reports have shown blue and green LED micro-displays using InGaN-on-sapphire LEDs [7–9] and InGaN-on-silicon LEDs [10–12]. Red LED micro-displays have also been presented using sapphire-bonded [13,14] and thin film AlGaInP red LED epi-layers [15]. Currently, monochromatic LED micro-display technologies have already realized $>$ 5,000 pixels per inch (PPI) with a pixel diameter of 2 µm [16]. In contrast, the progress of full-color LED micro-displays has been relatively unsatisfactory. There are significant technical challenges for full-color realization combining red/green/blue (R/G/B) LEDs that come from different epi-wafers [17,18]. Although transferring multiple individual LED chips in one go is a possible full-color solution, it is a yet to mature time-consuming process, associated with yield issues as the display and pixel sizes scale down and number of pixels increases [19].

Color conversion technology has been adopted for full-color LED micro-displays without the need of placing substantial numbers of R/G/B LED chips on the same driving substrate. A color conversion layer, containing red or green quantum dot (QD)-based materials, can be coated on the pixels of monochromatic blue LED micro-displays by inkjet printing or photolithography [20–22]. QD-based color conversion materials can reach 30% or higher conversion efficiency [23]. However, absorption of the pumping light is usually insufficient because of limited light extraction, aperture, and optical density of color conversion patterns. As a result, the luminance of the display is only $\sim 10^3$ cd/m^2 after applying color conversion layers as reported to date [20].

#459226 https://doi.org/10.1364/OE.459226
Journal © 2022 Received 23 Mar 2022; revised 27 May 2022; accepted 1 Jun 2022; published 13 Jun 2022

Optics EXPRESS

In addition, optical crosstalk is severe between LEDs and color conversion layers, significantly deteriorating the color purity [22]. The stability of QD-based materials [24] is also yet to be fully investigated, especially under large current and high luminance conditions where excessive heat is generated. Possible material degradations can affect the reliability of the color conversion in full-color LED micro-displays. All these issues of color conversion technology remain to be satisfactorily resolved.

Other approaches without color conversion have also been investigated. Works on full-color InGaN LEDs by tuning material growth [25] or by intentional wavelength shift [26] present inefficient emission intensity due to the difficulties in growing red emitting InGaN [27]. Heterogeneous integration of InGaN and AlGaInP LEDs, such as wafer stacking [28] and adhesive epi-layer bonding [29,30], are potential solutions for high-brightness full-color micro-displays. Nevertheless, it is challenging to integrate three different epitaxial layers of LEDs, and driving of the micro-displays is significantly complex. Thus, simplification of the integration process is highly desirable. Previously, we reported InGaN blue/green dual-wavelength LEDs grown and fabricated using the same monochromatic LED process [31,32]. Blue and green subpixels can be formed on the same epi-wafer so that the heterogeneous integration process for full-color micro-displays is greatly simplified. Only AlGaInP red LED arrays are required to be bonded by flip-chip technology [15] to the driving substrate with dual-wavelength LEDs for full-color realization.

Here, we report demonstration of a full-color LED micro-display using heterogeneous integration technology. The micro-display has 32×32 full-color pixels and a pixel pitch of 120 µm that consists of 40 µm × 120 µm R/G/B subpixels. The blue and green subpixels were monolithically fabricated using color filters (CFs) on InGaN dual-wavelength LED epi-wafers, and thin film AlGaInP red LED subpixel arrays were flip-chip bonded afterwards. The full-color LED micro-display is driven on a printed circuit board (PCB) using constant current driving. The full-color LED micro-display exhibits high brightness and a wide color gamut. Several graphics are shown to demonstrate the display feasibility. The results prove that this heterogeneous integration technology has a unique simplicity in manufacturing high-performance full-color LED micro-displays.

2. Fabrication of full-color LED micro-display

2.1. LED epi-wafers

InGaN blue/green dual-wavelength LED epi-layers were grown on a 2-inch c-plane sapphire substrate (450 µm thick) in our close-coupled showerhead (CCS) metal-organic chemical vapor deposition (MOCVD) system. The epi-structure (Fig. 1(a)) contains 0.8 µm undoped GaN, 3.0 µm n-GaN, 10 × GaN/InGaN shallow wells, 5 × GaN/InGaN multiple quantum wells (MQWs), a 50 nm electron blocking layer and 200 nm p-GaN grown sequentially on the sapphire substrate. The quantum well (QW) region has 3 × blue emission QWs at the bottom, 1 × green emission QW in between and 1 × blue emission QW on the top. The emission wavelength of the QWs is controlled by changing the growth temperature, while other growth parameters are kept identical. To obtain LEDs with comparable blue and green peaks, the top blue QW is necessary to balance the carrier injection into the blue and green QWs. Without the top blue QW, the LEDs show mainly green emission [33].

AlGaInP red LED epi-wafers are commercial wafers for flip-chip epi-down LEDs. The epi-layers were grown on a 4-inch (001) n-GaAs substrate (350 µm thick) by MOCVD. The epi-structure (Fig. 1(b)) has a 300 nm GaInP etch stop layer, 100 nm n-GaAs contact layer, 3.4 µm n-AlGaInP current spreading layer, 0.7 µm n-AlInP cladding layer, 0.5 µm AlGaInP QW active layer, 1.2 µm p-AlInP cladding layer and 2 µm p-GaP window layer, from the substrate to the top. The GaInP etch stop layer has a high selectivity when the absorbing GaAs substrate is removed by wet etching [34]. Note that the n-GaAs contact layer was grown originally for the

Optics EXPRESS

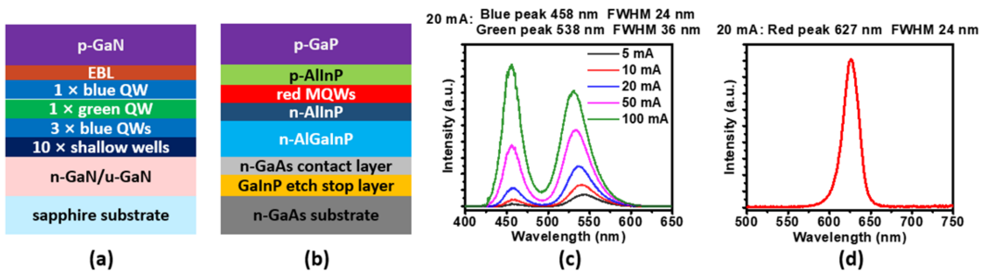

Fig. 1. Structures of (a) InGaN blue/green dual-wavelength and (b) AlGaInP red LED epi-wafers. EL spectra of (c) dual-wavelength and (d) red LEDs.

n-electrodes of vertical LEDs, and serves no purpose in our work due to a different electrode structure design in which n-electrodes are formed on the n-AlGaInP layer.

The electroluminescence (EL) spectra of InGaN dual-wavelength and AlGaInP red LEDs were measured using 320 µm-diameter circular devices. The EL spectra of a typical InGaN dual-wavelength LED at different current intensities are plotted in Fig. 1(c). At 20 mA (25 A/cm^2), the blue peak is at 458 nm with a full width at half maximum (FWHM) of 24 nm, and the green peak is at 538 nm with a FWHM of 36 nm. The two peaks are well-separated, which means that the undesired peak is easily filtered out by the blue/green CFs to form monochromatic subpixels. The blue emission becomes stronger with the increase of driving current, which is attributed to more hole injection into the three bottom blue QWs [35]. The EL spectrum of a typical AlGaInP red LED at 20 mA (25 A/cm^2) is shown in Fig. 1(d). The red peak is at 627 nm and the FWHM is 24 nm. All the R/G/B emission peaks have narrow FWHMs, presenting good monochromaticity.

2.2. Fabrication of dual-wavelength LED array

Blue and green subpixels for the full-color LED micro-displays were fabricated on the InGaN blue/green dual-wavelength LED epi-wafers, as shown in Fig. 2(a)–(d). Isolation trenches were etched in BCl_3-Cl_2 plasma using SiO_2 as a hard mask to form electrical isolation between subpixels. Subpixel mesas of 1 µm in height were then etched in the same way, and a 115 nm indium tin oxide (ITO) current spreading layer was deposited on top of the mesas. Each full-color pixel consists of two dual-wavelength subpixels and a blank area for red LED bonding. The size of the subpixels is 40 µm × 120 µm with an emitting area (mesa) of 23 µm × 97 µm. A Ti/Al/Ti/Au (20/200/50/50 nm) metal stack was deposited on the n-GaN layer as n-electrodes. Before p-electrode deposition, a red CF was filled into the isolation trenches to suppress optical crosstalk and a transparent overcoat photoresist was cured as an insulating layer [32] covering the n-electrodes. The p-electrodes are thicker than the n-electrodes (Ti/Cu/Ti/Au, 100/1500/20/20 nm) to reduce resistance, providing a more uniform driving current [32]. Finally, 1.5 µm-thick blue and green CFs were coated on the dual-wavelength subpixels for blue and green emission, respectively. The CF materials used in the fabrication are commercial colored photoresists widely used in flat panel displays. The bonding pads for the red subpixels were left open without any coating, as labelled in Fig. 2(e). The bonding pads for the n-electrodes are about 1.6 µm thicker than those for the p-electrodes, partially offsetting the mesa height difference of the AlGaInP red LED subpixels.

2.3. Fabrication of red LED array

Red subpixels for the full-color LED micro-displays were fabricated on AlGaInP red LED epi-wafers, as shown in Fig. 3(a)–(d). Similar to our previously reported work on red LED

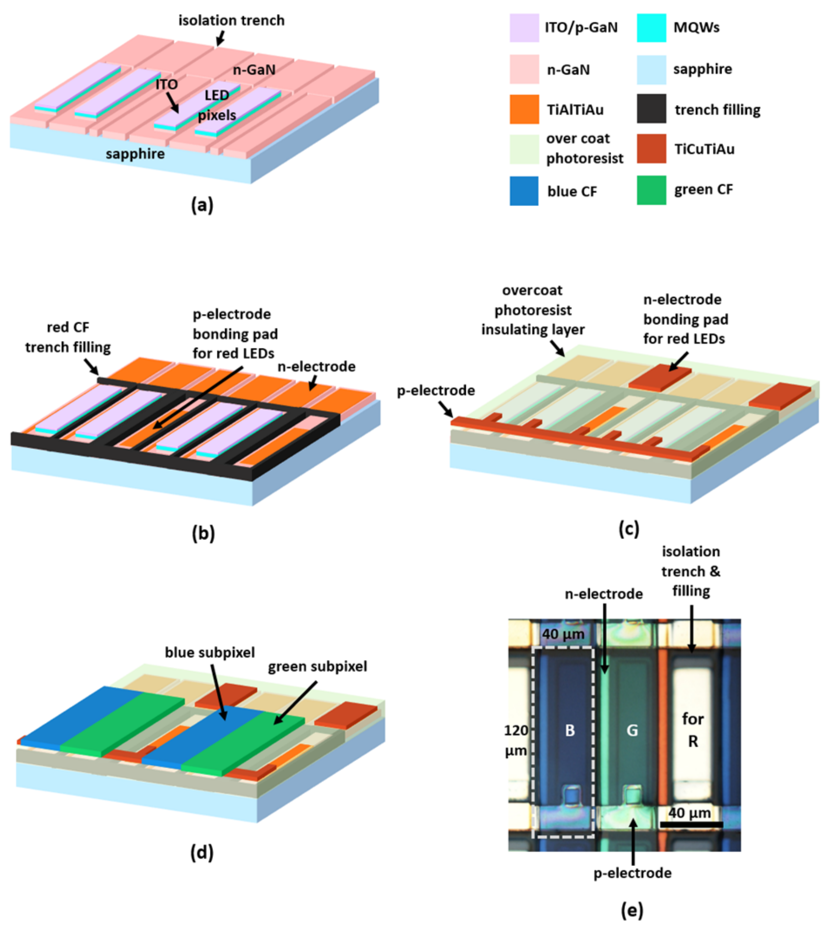

Fig. 2. The fabrication process of the dual-wavelength LED array: (a) etching of isolation trenches and pixels; (b) deposition of n-electrodes; (c) deposition of p-electrodes; (d) CF coating. Each layer is labelled according to the legend in the top right-hand corner (some epi-layers are omitted). (e) A photomicrograph of a full-color pixel (without red subpixels bonded) after the fabrication process.

micro-displays [15], 120 nm-thick Au p-electrodes were patterned, followed by the etching processes of the isolation regions and subpixel mesas in BCl_3-Cl_2-Ar plasma using SiO_2 masks. The mesa of each red subpixel is 27 µm × 114 µm with a height of 5 µm. Isolation regions are 7 µm-deep, and not fully etched away by dry etching at first. Since plasma dry etching of (Al)GaInP is non-selective to the GaAs substrate, the remaining n-AlGaInP/n-GaAs/GaInP layers in the isolation regions were removed by wet etching, using HCl-H_3PO_4, diluted H_3PO_4-H_2O_2, and HCl-H_3PO_4 in sequence [36]. These isolation regions also work as transparent window regions (to be discussed in Section 3.1). Ge/Au/Ni/Au (40/40/24/100 nm) n-electrodes were deposited on the n-AlGaInP. After electrode fabrication, 1 µm-thick SiO_2 was coated as a passivation layer to protect the red LED subpixels, and as an etch stop layer in the isolation regions. Contact holes of 10 µm in diameter were subsequently etched on the n- and p-electrodes. Around 6 µm-thick bisbenzocyclobutene (BCB) was filled into the surrounding mesas by spin-coating and etched back in O_2-CF_4 plasma, as BCB can improve the mechanical strength of the thin film red LED array. Finally, 2 µm-thick In patterns were deposited on the contact holes by thermal evaporation.

Optics EXPRESS

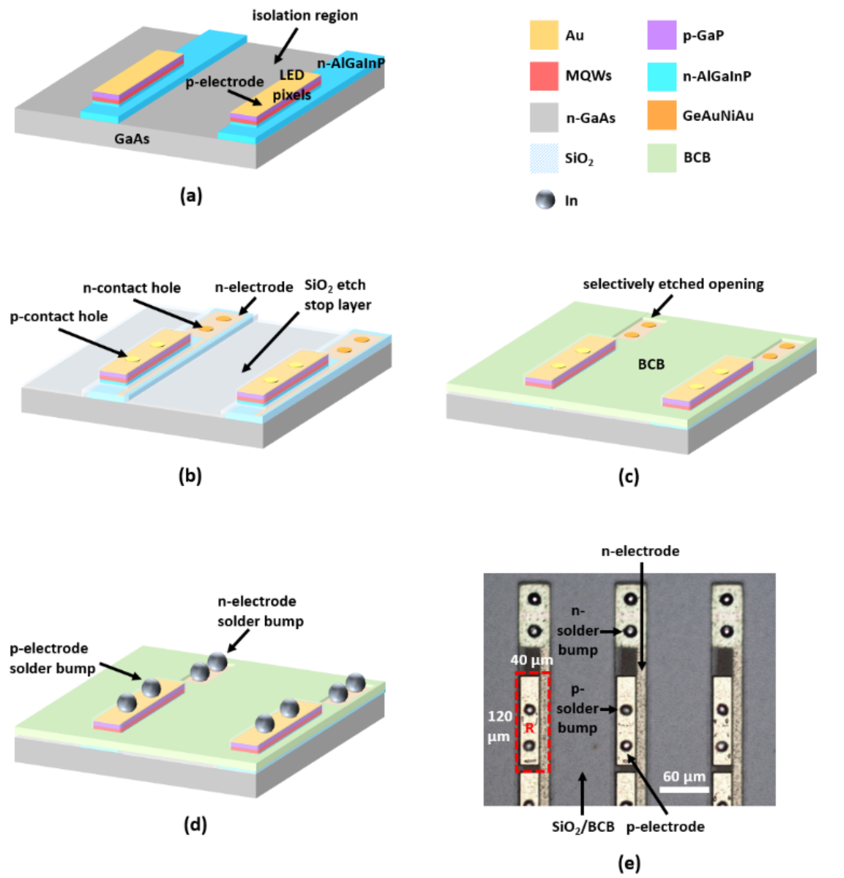

Fig. 3. The fabrication process of the red LED array: (a) etching of isolation regions and pixels; (b) deposition of n-electrodes and a SiO_2 passivation/etch stop layer; (c) BCB filling and etching; (d) formation of In solder bumps. Each layer is labelled according to the legend in the top right-hand corner (some epi-layers are omitted). (e) A photomicrograph of red LED subpixels after the fabrication process.

With the help of water-soluble flux, the In patterns were reshaped into 10 μm-high solder bumps by the reflow process at 230 for 10 s on the hotplate. A photomicrograph of the red LED array before bonding is given in Fig. 3(e).

2.4. Heterogeneous integration

Chip-level heterogeneous integration is conducted for full-color realization. The size of the dual-wavelength LED chip is 8.92 mm × 6.60 mm and the size of the red LED chip is 4.24 mm × 4.46 mm. The display area is 3.84 mm × 3.84 mm (32 × 32 resolution with a 120 μm full-color pixel pitch) on the dual-wavelength LED chip. The red LED chip was flip-chip bonded onto the display area of the dual-wavelength LED chip by Au/In bonding. A manual flip-chip bonder with a placement accuracy of 0.5 μm was utilized to align and place the chips. Afterwards, the chips were heated to 230 °C from the ambient temperature at a ramp rate of 4 °C/s under a 200 N bonding force and the temperature was kept for 2 minutes (Fig. 4(a)). Indium solder bumps on the p-electrodes were pressed flat above the eutectic temperature during the bonding, and thus 10 μm solder bumps are sufficient to fill the gap between the n-electrodes of the red LEDs and n-bonding pads on the dual-wavelength LED chip.

Optics EXPRESS

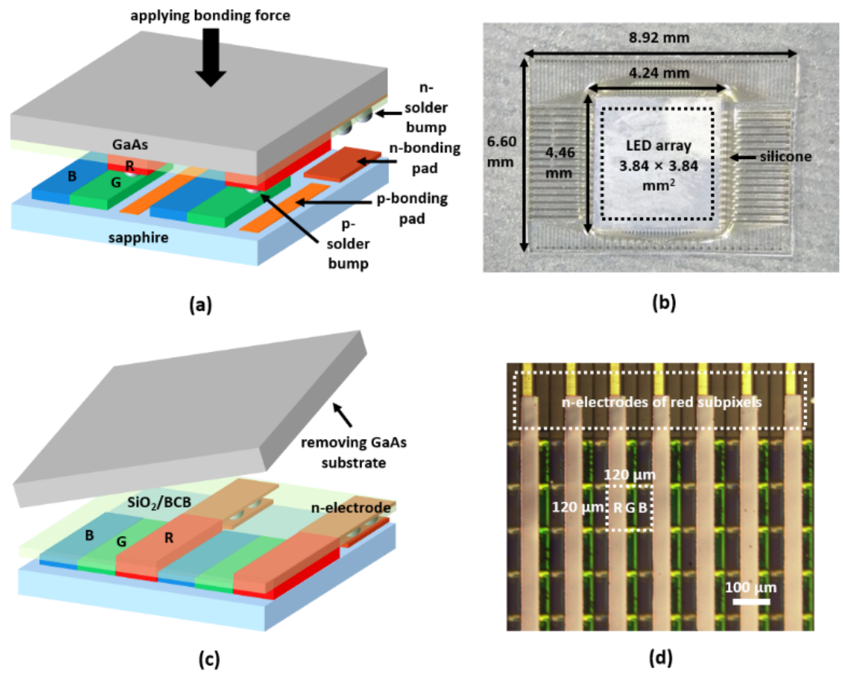

Fig. 4. (a) A diagram of the flip-chip bonding process. (b) A photo of the LED micro-display chip with silicone protection before removing the GaAs substrate. (c) A diagram of the GaAs substrate removal process. (d) A photomicrograph of R/G/B subpixel arrays after the heterogeneous integration process. (Some structures of the micro-display chip are omitted in diagrams (a) and (c))

After bonding, the periphery of the red LED chip was sealed with silicone, cured at 120 °C for 2 hours. A photo of the LED micro-display chip after silicone curing is shown in Fig. 4(b), with the chip size labelled. Silicone not only prevents the underlying pixels from being damaged in the wet etching of the GaAs substrate, but also provides extra support to the edge of thin film red LEDs to avoid deformation and cracking. Photoresist was coated on other areas of the dual-wavelength LED chip to protect the metals. The 350 μm-thick GaAs substrate covering the red LED subpixels was then totally removed in ammonia-H_2O_2 (Fig. 4(c)). The substrate etching was terminated at the GaInP/GaAs interface (in red subpixel regions) or the SiO_2/GaAs interface (in isolation regions) with a high etching selectivity. The photomicrograph of the LED micro-display chip after removal of the substrate is shown in Fig. 4(d). The entire AlGaInP red LED array with SiO_2/BCB filling was finally uniformly bonded next to the blue/green subpixels on the dual-wavelength LED chip. The small overlap between red and green subpixel columns is due to the lateral misalignment of the two chips, which can be optimized by enlarging the window regions on the red LED array. Full-color emission is easily realized on this heterogeneous LED micro-display by driving the addressable R/G/B subpixels.

3. Characterization and discussion

3.1. SiO_2/BCB composite layer in window regions

In the heterogeneous full-color LED micro-display, the thin film AlGaInP red LED layer is placed on top of the InGaN blue/green dual-wavelength LED layer, and transparent window regions in the red LED layer above the underlying blue/green subpixels are formed. Otherwise, the absorbing AlGaInP-based epi-layers would block all blue/green light emission. In the design of the AlGaInP chip, the isolation regions between the red LEDs (labelled in Fig. 3(a)) are the transparent window regions, which were previously defined in the chip fabrication process. All semiconductor epi-layers in these regions were removed, including the GaInP etch stop layer. However, these window regions cannot be left without any protection in the substrate wet etching process. Without an etch stop layer, ammonia-H_2O_2 etchant would flow through the window regions, destroying all underlying metal connections and subpixels during the removal process of the GaAs substrate.

To prevent damage from the etchants, a transparent SiO_2/BCB composite layer was filled into the window regions as an etch stop layer between the red LED subpixels: a 1 µm-thick SiO_2 layer was first deposited and a 6 µm thick BCB layer was then filled in. Substrate wet etching would stop at the surface of the SiO_2/BCB composite layer with a high selectivity and etchants cannot penetrate through this layer. Although both SiO_2 and BCB do not react with the ammonia-H_2O_2 substrate etchant, it is not preferable to solely coat a single layer of either SiO_2 or BCB as the etch stop layer. A single layer of 1 µm-thick SiO_2 is fragile, especially in the window regions where no solder bumps provide mechanical support. The residual stress induced by the flip-chip bonding can easily break the SiO_2 layer during the substrate etching process. A single layer of 6 µm-thick BCB, meanwhile, has enough mechanical strength, but the adhesion to semiconductor sidewalls is not as firm as that of SiO_2. During removal of the substrate, etchants attack the BCB/semiconductor interface and finally cause the BCB layer to fall off. The SiO_2/BCB composite etch stop layer avoids these pitfalls: SiO_2 provides reliable sidewall adhesion and BCB enhances the strength of the whole thin film array. This composite structure in the window regions plays a key role in the heterogeneous integration technology.

Figure 5(a) is a cross-sectional scanning electron microscope (SEM) image of the semiconductor/SiO_2/BCB interface on the GaAs substrate. Prior to the deposition of SiO_2, all semiconductor epi-layers in the window regions were removed by wet etching and the smooth surface of the GaAs substrate was exposed. A rough surface or etching residue on the GaAs will greatly compromise the adhesion and integrity of the deposited SiO_2, which could fail to resist etchants in the substrate wet etching process. In our work, the interface between the 1 µm-thick SiO_2 layer and the GaAs substrate is defect-free. The SiO_2 also has a full step coverage on the sidewall of the red LED subpixels. At the same time, the 6 µm-thick BCB layer adheres well to the SiO_2 layer at both the window regions and the sidewall. The rough BCB surface originated from the O_2-CF_4 plasma etching can be further optimized. Figure 5(b) shows the semiconductor/SiO_2/BCB interface after flip-chip bonding and removal of the substrate. The top SiO_2 layer sticks well to the adjacent GaInP, forming an entire etch stop layer to protect the underlying subpixels. The defect-free morphology and sidewall adhesion of the SiO_2/BCB composite layer is retained after substrate etching, proving a sufficient etching resistance and high stability.

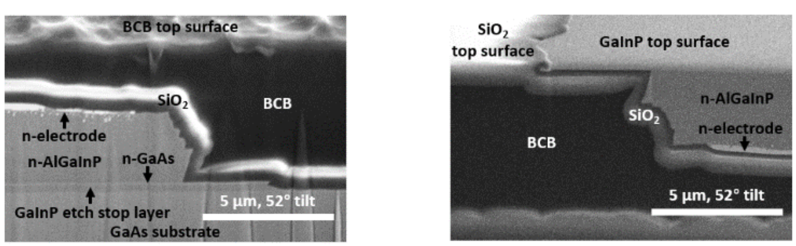

(a) (b)

Fig. 5. Cross-section SEM images of the AlGaInP red LED chip showing the SiO_2/BCB composite layer: (a) on the GaAs substrate; (b) after removal of the GaAs substrate.

Optics EXPRESS

3.2. Characterization of full-color micro-display

Typical *I-V* characteristics of single R/G/B subpixels (Fig. 6(a)) were measured using a probe station after all the fabrication processes. All three kinds of subpixels exhibit low reverse leakage current (< 1 nA) at −5 V, which indicates few defects in the epi-layers and LED sidewalls. The forward voltages of the R/G/B subpixels at 25 A/cm^2 are 2.04 V, 3.51 V and 3.46 V, respectively. The blue and green subpixels have similar electrical characteristics since they were fabricated from the same dual-wavelength LED epi-wafer. The full-color micro-display is driven on a PCB by a commercial passive-matrix LED display controller, and has a resolution of 32×32, containing 32 rows and 96 columns ($32 \times$ R/G/B subpixels). All LED subpixels within each row share the same p-electrode, and subpixels within each column share the same n-electrode. Row scan signals of 5 V are applied to the p-electrodes via a 5–32 decoder that is made from 3–8 decoders (SM5166P) and inverters (74HC04). The n-electrodes are connected to the constant current LED sink driver chips (MBI5026) that can adjust the output current by external resistors. The driving current of each green and red subpixel is set to 1 mA, while that of each blue subpixel is 2 mA. The higher driving current of blue subpixels satisfies the luminance requirement for color mixing. The current density of the R/G/B subpixels is 32 A/cm^2, 45 A/cm^2 and 90 A/cm^2, and the corresponding forward voltage is 2.12 V, 3.84 V and 4.43 V, respectively. All subpixels have low enough voltages to be driven under the 5 V scan signals. The full-color micro-display is driven at a frame rate of 120 frames per second. The scan duration of each row is 1/32 of the frame duration (1/32 scan mode) and the maximum power consumption of the LED array on the micro-display chip is 0.5 W.

Figure 6(b) shows the EL spectra of full-screen R/G/B monochromatic emissions from the full-color micro-display. The green and red emissions from the micro-display are relatively pure, while the blue emission has some green leakage. Figure 6(c) shows the transmittance spectra of 1.5 µm-thick blue and green CFs coated on the dual-wavelength LEDs. The color purity of blue emission is limited by the absorption blue CF material, which is insufficient at the wavelength shorter than 540 nm [37]. The peak wavelengths of the R/G/B emissions are 629 nm, 531 nm and 447 nm. Their CIE 1931 color space coordinates (x, y) are (0.70, 0.30), (0.21, 0.69) and (0.15, 0.14), respectively. The blue point slightly shifts to the green side because of the green leakage from blue subpixels, and this issue can be solved by coating thicker CF or increasing the optical density of CF. The chromaticity diagram of the EL spectra indicates that the color gamut of the full-color micro-display is comparable with that of standard RGB (Fig. 6(d)). A full-screen white pattern with color coordinates (x, y) of (0.30, 0.29) was demonstrated after tuning the brightness of the R/G/B subpixels. Figure 6(e) is the photos of the R/G/B and white colors shown on the micro-display chip. The luminance of the micro-display showing full-screen white color (0.30, 0.29) is 6.4×10^3 cd/m^2 at 1/32 scan driving. It is possible to reach a luminance over 10^5 cd/m^2 using active-matrix driving with a higher driving duty ratio. Figure 6(f) presents examples of full-color images shown on the micro-display. It can appropriately reproduce colors and details of original images. No short nor open circuit line exists, and some dead pixels are attributed to unsatisfactory sidewall coating of p-electrodes due to the limitations of the process equipment. All photos of the micro-display in Fig. 6(e) and Fig. 6(f) were captured at an exposure time of 1/20 s, and the brightness of the micro-display was set to 10% to prevent over-exposure of photos. Specifications of the heterogeneous full-color LED micro-display are summarized in Table 1.

Optics EXPRESS

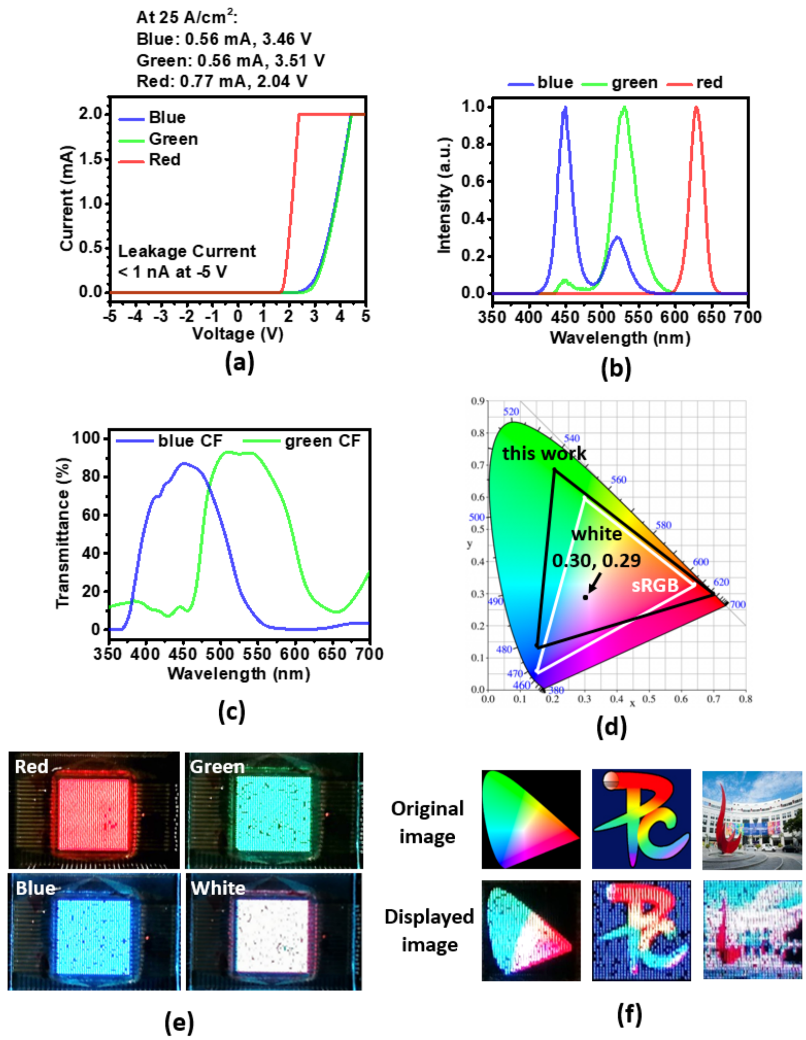

Fig. 6. (a) I-V characteristics of a single R/G/B subpixel. (b) EL spectra of the LED micro-display showing R/G/B colors. (c) Transmittance spectra of 1.5 μm-thick blue and green CFs. (d) The CIE 1931 color space coordinates (x, y) of R/G/B colors and color gamut of the LED micro-display. (e) Photos of the LED micro-display showing R/G/B and white colors. (f) Original full-color images and their corresponding demonstration on the micro-display.

Table 1. Specifications of the heterogeneous full-color LED micro-display

Item	Specification
Chip Size	8.92 mm × 6.60 mm
Screen Size	3.84 mm × 3.84 mm
Resolution	32 × 32 × RGB
Pixel Pitch	120 µm (subpixel: 40 µm × 120 µm)
Pixel Density	212 PPI
Fill Factor	52%
CIE 1931 Color Space Coordinates (x, y)	red: (0.70, 0.30) green: (0.21, 0.69) blue: (0.15, 0.14)
Brightness	6.4×10^3 cd/m^2 (full-screen white color)
Driving Method	passive-matrix, 1/32 scan
Power Consumption	≤ 0.5 W (LED array)

4. Conclusion

A full-color LED micro-display was fabricated by heterogeneous integration of InGaN blue/green dual-wavelength and AlGaInP red LED arrays. The InGaN dual-wavelength LED epi wafers were grown on sapphire substrates and commercial AlGaInP red LEDs on GaAs substrates. Both dual-wavelength and red LEDs were monolithically fabricated on the native epi-wafers using microelectronic fabrication technologies. Blue and green LED subpixels on the dual-wavelength LED chip were realized by coating blue and green CFs and driven at different current densities. The red LED chip was flip-chip bonded to the dual-wavelength LED chip using indium solder bumps. Subsequently, its GaAs substrate was removed by wet etching, leaving addressable thin film red LED subpixels. Blue and green light are transmitted through window regions of the thin film red LED array, where semiconductor epi-layers removed previously were filled with a transparent SiO_2/BCB composite layer. The full-color LED micro-display has a resolution of 32 × 32 full-color pixels, and each pixel has a 120 µm pitch consisting of 40 µm × 120 µm R/G/B subpixels. All three kinds of subpixels show acceptable forward voltages and low reverse leakage currents. Constant current 1/32 scan passive-matrix driving is adopted for the full-color LED micro-display. Panel-level characterization proves that the micro-display has a wide color gamut comparable to that of standard RGB, and the full-screen white emission from the micro-display exhibits 6.4×10^3 cd/m^2 luminance at a power consumption of no more than 0.5 W. Image demonstration with a wide color gamut on the full-color micro-display illustrates that it is a feasible and cost-effective technology to produce high-performance full-color LED micro-displays. Based on this full-color micro-display prototype, the pixel pitch can be further reduced to less than 20 µm for practical VR/AR devices [38] in the future. This heterogeneous integration technology also shows the potential for active-matrix driven micro-displays, by sequential flip-chip bonding of a dual-wavelength LED array and a red LED array on an active-matrix driver chip. In this case, using dual-wavelength LEDs still helps to simplify the fabrication procedures and reduce the cost, in contrast with bonding blue and green LED arrays on the driver chip separately.

Funding. Innovation and Technology Commission (ITS/120/20).

Disclosures. The authors declare that there is no conflict of interest.

Data availability. Data underlying the results presented in this paper are not publicly available at this time but may be obtained from the authors upon reasonable request.

Optics EXPRESS

References

1. T. Zhan, K. Yin, J. Xiong, Z. He, and S. Wu, "Augmented Reality and Virtual Reality Displays: Perspectives and Challenges," iScience **23**(8), 101397 (2020).
2. G. Haas, "40-2: Invited Paper: Microdisplays for Augmented and Virtual Reality," Dig. Tech. Pap. - SID Int. Symp. **49**(1), 506–509 (2018).
3. T. Wu, C. Sher, Y. Lin, C. Lee, S. Liang, Y. Lu, S. Huang Chen, W. Guo, H. Kuo, and Z. Chen, "Mini-LED and Micro-LED: Promising Candidates for the Next Generation Display Technology," Appl. Sci. **8**(9), 1557 (2018).
4. Y. Huang, E. Hsiang, M. Deng, and S. Wu, "Mini-LED, Micro-LED and OLED displays: present status and future perspectives," Light: Sci. Appl. **9**(1), 105 (2020).
5. E. Hsiang, Z. Yang, Q. Yang, Y. Lan, and S. Wu, "Prospects and challenges of mini-LED, OLED, and micro-LED displays," J. Soc. Inf. Disp. **29**(6), 446–465 (2021).
6. Z. Yang, E. Hsiang, Y. Qian, and S. Wu, "Performance Comparison between Mini-LED Backlit LCD and OLED Display for 15.6-Inch Notebook Computers," Appl. Sci. **12**(3), 1239 (2022).
7. H. X. Jiang, S. X. Jin, J. Li, J. Shakya, and J. Y. Lin, "III-nitride blue microdisplays," Appl. Phys. Lett. **78**(9), 1303–1305 (2001).
8. J. Day, J. Li, D. Y. C. Lie, C. Bradford, J. Y. Lin, and H. X. Jiang, "III-Nitride full-scale high-resolution microdisplays," Appl. Phys. Lett. **99**(3), 031116 (2011).
9. C. Chen, H. Chen, J. Liao, C. Yu, and M. Wu, "Fabrication and Characterization of Active-Matrix 960×540 Blue GaN-Based Micro-LED Display," IEEE J. Quantum Electron. **55**(2), 1–6 (2019).
10. X. Zhang, P. Li, X. Zou, J. Jiang, S. H. Yuen, C. W. Tang, and K. M. Lau, "Active Matrix Monolithic LED Micro-Display Using GaN-on-Si Epilayers," IEEE Photonics Technol. Lett. **31**(11), 865–868 (2019).
11. C. J. Hun, S. J. Lee, K. O. Kwon, J. Y. Choi, T. Jung, M. Han, and S. J. Han, "A monolithically integrated micro-LED display based on GaN-on-silicon substrate," Appl. Phys. Express **13**(2), 026501 (2020).
12. L. Qi, X. Zhang, W. C. Chong, P. Li, and K. M. Lau, "848 ppi high-brightness active-matrix micro-LED micro-display using GaN-on-Si epi-wafers towards mass production," Opt. Express **29**(7), 10580–10591 (2021).
13. Z. J. Liu, W. C. Chong, K. M. Wong, and K. M. Lau, "360 PPI Flip-Chip Mounted Active Matrix Addressable Light Emitting Diode on Silicon (LEDoS) Micro-Displays," J. Display Technol. **9**(8), 678–682 (2013).
14. R. Horng, H. Chien, F. Tarntair, and D. Wuu, "Fabrication and Study on Red Light Micro-LED Displays," IEEE J. Electron Devices Soc. **6**, 1064–1069 (2018).
15. P. Li, X. Zhang, W. C. Chong, and K. M. Lau, "Monolithic Thin Film Red LED Active-Matrix Micro-Display by Flip-Chip Technology," IEEE Photonics Technol. Lett. **33**(12), 603–606 (2021).
16. L. Zhang, F. Ou, W. C. Chong, Y. Chen, and Q. Li, "Wafer-scale monolithic hybrid integration of Si-based IC and III–V epi-layers—A mass manufacturable approach for active matrix micro-LED micro-displays," J. Soc. Inf. Disp. **26**(3), 137–145 (2018).
17. X. Zhou, P. Tian, C. Sher, J. Wu, H. Liu, R. Liu, and H. Kuo, "Growth, transfer printing and colour conversion techniques towards full-colour micro-LED display," Prog. Quantum Electron. **71**, 100263 (2020).
18. Y. Wu, J. Ma, P. Su, L. Zhang, and B. Xia, "Full-Color Realization of Micro-LED Displays," Nanomaterials **10**(12), 2482 (2020).
19. E. H. Virey, N. Baron, and Z. Bouhamri, "11-3: Overlooked Challenges for microLED Displays," SID Symposium Digest of Technical Papers **50**(1), 129–132 (2019).
20. H. Onuma, M. Maegawa, T. Kurisu, T. Ono, S. Akase, S. Yamaguchi, N. Momotani, Y. Fujita, Y. Kondo, K. Kubota, T. Yoshida, Y. Ikawa, T. Ono, H. Higashisaka, Y. Hirano, and H. Kawanishi, "25-5: Late-News Paper: 1,053 ppi Full-Color "Silicon Display" based on Micro-LED Technology," Dig. Tech. Pap. - SID Int. Symp. **50**(1), 353–355 (2019).
21. T. Xuan, S. Shi, L. Wang, H. Kuo, and R. Xie, "Inkjet-Printed Quantum Dot Color Conversion Films for High-Resolution and Full-Color Micro Light-Emitting Diode Displays," J. Phys. Chem. Lett. **11**(13), 5184–5191 (2020).
22. X. Zhang, L. Qi, W. C. Chong, P. Li, C. W. Tang, and K. M. Lau, "Active matrix monolithic micro-LED full-color micro-display," J. Soc. Inf. Disp. **29**(1), 47–56 (2021).
23. C. Chen, K. Chen, and R. Chiang, "62-1: High-Resolution Quantum-Dot Photoresist for Full-Color μ-LED Microdisplays," SID Symposium Digest of Technical Papers **52**(1), 884–887 (2021).
24. H. Moon, C. Lee, W. Lee, J. Kim, and H. Chae, "Stability of Quantum Dots, Quantum Dot Films, and Quantum Dot Light-Emitting Diodes for Display Applications," Adv. Mater. **31**(34), 1804294 (2019).
25. H. S. El-Ghoroury, M. Yeh, J. C. Chen, X. Li, and C. Chuang, "Growth of monolithic full-color GaN-based LED with intermediate carrier blocking layers," AIP Adv. **6**(7), 075316 (2016).
26. K. Chung, J. Sui, B. Demory, and P. Ku, "Color mixing from monolithically integrated InGaN-based light-emitting diodes by local strain engineering," Appl. Phys. Lett. **111**(4), 041101 (2017).
27. B. Damilano and B. Gil, "Yellow-red emission from (Ga,In)N heterostructures," J. Phys. D: Appl. Phys. **48**(40), 403001 (2015).
28. K. Yadavalli, C. Chuang, and H. S. El-Ghoroury, "Monolithic and heterogeneous integration of RGB micro-LED arrays with pixel-level optics array and CMOS image processor to enable small form-factor display applications," Proc. SPIE **11310**, 78 (2020).

Optics EXPRESS

29. C. Kang, J. Lee, D. Kong, J. Shim, S. Kim, S. Mun, S. Choi, M. Park, J. Kim, and D. Lee, "Hybrid Full-Color Inorganic Light-Emitting Diodes Integrated on a Single Wafer Using Selective Area Growth and Adhesive Bonding," ACS Photonics **5**(11), 4413–4422 (2018).
30. S. Mun, C. Kang, J. Min, S. Choi, W. Jeong, G. Kim, J. Lee, K. Kim, H. C. Ko, and D. Lee, "Highly Efficient Full-Color Inorganic LEDs on a Single Wafer by Using Multiple Adhesive Bonding," Adv. Mater. Interfaces **8**(14), 2100300 (2021).
31. Y. D. Qi, H. Liang, W. Tang, Z. D. Lu, and K. M. Lau, "Dual wavelength InGaN/GaN multi-quantum well LEDs grown by metalorganic vapor phase epitaxy," J. Cryst. Growth **272**(1-4), 333–340 (2004).
32. P. Li, X. Zhang, Y. Li, L. Qi, C. W. Tang, and K. M. Lau, "Monolithic full-color microdisplay using patterned quantum dot photoresist on dual-wavelength LED epilayers," J. Soc. Inf. Disp. **29**(3), 157–165 (2021).
33. Y. Jiang, Y. Li, Y. Li, Z. Deng, T. Lu, Z. Ma, P. Zuo, L. Dai, L. Wang, H. Jia, W. Wang, J. Zhou, W. Liu, and H. Chen, "Realization of high-luminous-efficiency InGaN light-emitting diodes in the "green gap" range," Sci. Rep. **5**(1), 10883 (2015).
34. R. H. Horng, S. Sinha, C. P. Lee, H. A. Feng, C. Y. Chung, and C. W. Tu, "Composite metal substrate for thin film AlGaInP LED applications," Opt. Express **27**(8), A397–A403 (2019).
35. M. V. Kisin, D. V. Mamedov, and H. S. El-Ghoroury, "Simulation of full-color III-nitride LED with intermediate carrier blocking layers," Opt. Quantum Electron. **48**(12), 525 (2016).
36. A. R. Clawson, "Guide to references on III–V semiconductor chemical etching," Mater. Sci. Eng. R Rep. **31**(1-6), 1–438 (2001).
37. H. Chen, R. Zhu, J. He, W. Duan, W. Hu, Y. Lu, M. Li, S. Lee, Y. Dong, and S. Wu, "Going beyond the limit of an LCD's color gamut," Light: Sci. Appl. **6**(9), e17043 (2017).
38. J. Xiong, E. Hsiang, Z. He, T. Zhan, and S. Wu, "Augmented reality and virtual reality displays: emerging technologies and future perspectives," Light: Sci. Appl. **10**(1), 216 (2021).